INTERCOMPARISON OF GLOBAL RESEARCH AND OPERATIONAL FORECASTS

Jennifer C. Roman
University of Utah, Salt Lake City, Utah

Gonzalo Miguez-Macho
Rutgers University, New Brunswick, New Jersey

Lee A. Byerle and Jan Paegle *
University of Utah, Salt Lake City, Utah

1. INTRODUCTION

A number of atmospheric forecast models have been developed and now display considerable skill in weather prediction. The underlying philosophy of these developments is that improved models and more accurate initial conditions should provide better forecasts. The importance of specific model improvements relative to specific observational enhancements may, nonetheless, still be inadequately understood. White et al. (1999) addressed some of these questions, and suggested the error spread among models of very different configuration and resolution is generally less than the magnitude of the error in any single relatively advanced model. Increased resolution in regional models does lead to some improvement in skill, particularly for heavier categories of precipitation that are not simulated at coarser resolution (White et al. 1999), and recent studies show improvement in wind forecasts due to enhanced model resolution (Hart 2004). This benefit, however, appears to be relatively small for other forecast variables, and is evident only for short-term forecasts in which point validations are made against observations, even in the most highly resolved and dynamically sophisticated approaches.

Various hypotheses have been proposed to explain this result. Some of these note current observing systems contain inadequate resolution of local regions of pronounced dynamic instability. Other explanations of the marginally superior performance of high-resolution models point to the evident difficulties in the validation of forecast features against coarsely spaced observations. All but one of the models studied by White et al. (1999) were limited area models and these are known to be strongly influenced by lateral boundary conditions supplied at their perimeter (Warner et al. 1997; Paegle et al. 1997). The Medium Range Forecast (MRF) model was the only global model evaluated by White et al. (1999) and that model also provided, or strongly influenced, the lateral boundary conditions of the tested limited area models.

The initial stages of the present research compared two global models [the Utah Global Model (UGM) and the MRF], and followed a hypothesis suggested by Miguez-Macho and Paegle (2000, henceforth MMP). This perspective, which is based upon downscale uncertainty growth, is supported by MMP and by Miguez-Macho and Paegle (2001), and is rooted in the early barotropic model predictability studies of Thompson (1957) and Lorenz (1969). Results obtained by MMP contrast with other recent literature emphasizing the importance of relatively smaller-scale instabilities (e.g,. Palmer et al. 1998; Hartmann et al. 1995) of the initial state, and other local error sources (e.g., Rabier et al. 1996). These perspectives and contrasting theories are summarized by MMP, who presented preliminary work suggesting that the dominant source of short-term forecast errors may be the uncertainty of relatively large scales of the initial state.

The present research extends MMP's studies to sort out the relative roles of the model resolution and initial state uncertainty and continues to probe the limitation to deterministic weather prediction due to inadequate observation of relatively large scales of the atmosphere. Other global model studies attempting to prioritize the relative contributions of initial errors, boundary errors, and model errors to total forecast error include work by Reynolds et al. (1994) and Hacker et al. (2003). Simmons and Hollingsworth (2002) show substantial improvement in forecast accuracy in global operational models over the past decade, and present an extensive list of forecast system changes that may have contributed to forecast improvement over the past two decades.

Initially, we sought to compare UGM and MRF forecasts in more detail. Our preliminary studies of

* *Corresponding author address*: Jan Paegle, University of Utah, Department of Meteorology, 135 South, 1460 East, Room 819, Salt Lake City, UT 84112-0110;
email: jpaegle@met.utah.edu

this problem focused on a 17-case forecast sample during boreal winter 1993, and compared research model forecasts executed at horizontal wavenumber 42 triangular truncation with MRF forecasts at horizontal wavenumber 62 triangular truncation. Those results were consistent with the possibility that uncertainty of the initial state represented the greatest limitation to forecast accuracy and implied that details of the model formulation were not equally important. (Note: results from studies not included in this extended abstract are available in Roman et al. 2004)

The UGM retains lower horizontal resolution and fewer levels than the MRF model, and has undergone much less extensive development and calibration. Regardless, comparisons of bias-corrected 500-mb geopotential height anomaly correlations (not shown here) reveal that UGM predictive skill lags that of the MRF by only 12 hours, and both show similar skill after seven days when the anomaly correlations drops below 0.6 for each model. When model-to-model anomaly correlations are calculated, those values are higher than the anomaly correlations of either model with analyses; therefore, the research model anticipates the MRF model evolution about as well as either model anticipates the real atmosphere. The fact that a relatively unsophisticated and more crudely resolved model possesses such high skill in anticipating the behavior of a much more sophisticated model implies that something other than model complexity provides the fundamental limitation in forecast accuracy for this set of 17 individual cases of the boreal winter of 1993. A possible inference is that both models suffer from the common deficiencies of imperfect initial state specification, and this may represent the primary forecast limitation for these cases. This inference carries important implications for deployment of observing systems and for forecast model development, and merits close scrutiny.

Therefore, we continue past studies by MMP of the rate of growth of the initial state uncertainty. MMP's experiments were limited by a couple of factors. First, they were integrated for only five days, and it was not possible to establish the timescale on which the uncertainty saturates. Second, the integrations were performed at a relatively coarse wavenumber 42 resolution, which could have limited error growth.

Consequently, a series of further predictability studies with the UGM is performed, with experiments to address each of these issues. In particular, all wavenumber 42 UGM experiments performed by MMP are now extended from five-day to two-week duration. Additionally, UGM cases from 1993 and 2003 are repeated at wavenumber 84 truncation to determine the influence of increased horizontal resolution upon forecast skill and sensitivity to initial state uncertainty.

The study is organized as follows. Section 2 presents brief overviews of the UGM and datasets. Section 3 studies sensitivity to initial state uncertainty for model runs at low resolution and section 4 illustrates the impact of doubled horizontal resolution on sensitivity to initial state uncertainty for the UGM. Section 5 presents overall conclusions.

2. DATASETS AND MODEL

a. Datasets

Both NCEP (Kalnay et al. 1996), in collaboration with NCAR, and the ECMWF (Gibson et al. 1997) have performed gridded retrospective analyses, based upon all available observations, by a frozen state-of-the-art global data assimilation system. Present estimates of initial state uncertainty for the cases from boreal winter 1993 are obtained from the difference of these two equally credible analyses and are assumed to be reasonable for this study. However, it is likely that this method of characterizing initial state uncertainty underestimates actual values at all scales. In fact, NCEP-NCAR reanalyses have been truncated at wavenumber 36, and, to the degree that ECMWF and NCEP-NCAR use the same observations, the difference in their analyses will underestimate the total error. This limitation to the study is further discussed in section 3.

The 17 cases previously used by MMP were selected for model initialization. These start on 1 January 1993, and continue at five-day intervals through March 1993. The particular dates are chosen because eight-day predictions by the version of the MRF used in the reanalyses are available within the NCEP-NCAR reanalysis archive. This allows comparison of the UGM research model with the MRF model, which is well documented within NCEP technical reports.

In addition to the earlier 1993 ensemble, a set of 15 cases was selected from boreal winter 2002/03 for high-resolution UGM model initialization. NCEP-NCAR reanalyses were utilized for these dates, as well as operational NCEP Global Data Assimilation System (GDAS) analyses that were available in near-real time. These analyses are

archived at 2.5° resolution on 26 vertical levels. Again, present estimates of initial state uncertainty for the cases from boreal winter 2002/03 are obtained from the difference of these two equally credible analyses and are assumed to be reasonable for this study. Because the high-resolution UGM time step is one-third that of the low-resolution UGM, larger sample sizes were not possible due to computational considerations.

b. Model

The UGM is based upon Galerkin approximations applied separately in each spatial dimension. Latitude and vertical structure are depicted by finite elements and longitude variability by Fourier series. The method retains the high accuracy and conservative properties of alternative Galerkin approximations, such as those used in the MRF that are based upon spherical harmonic expansions.

The dynamical core of the model uses a hydrostatic set of primitive equations in which vorticity, divergence, and thermal fields are predicted on pressure-based sigma coordinates. This approach is similar to that used in global models in operational centers, with the exception of numerical methods outlined above. Model physical parameterizations of convective and stable precipitation are similar to those used by the NCAR Community Climate Model 1 (Bath et al. 1987) introduced in 1987, and parameterizations of radiative and surface processes are also relatively less advanced and follow methods that have been used by other models more than two decades ago. Vertical mixing coefficients are calculated from a low-order turbulent energy equation, and radiation processes include cloud radiation interactions, as described for another model by Nicolini et al. (1993). Moist convective processes use simple convective adjustment, and cloud fraction and condensation criteria are based upon local relative humidity without explicit treatment of cloud microphysics. Sea surface temperature is maintained at the initial value, and land surface evaporation is extracted from the daily analysis files. Present applications retain 20 vertical levels and wavenumber 42 resolution. High-resolution experiments were repeated at wavenumber 84 resolution.

The UGM was originally designed by Paegle (1989) to address predictability questions. It has been used to study impact of wind data voids on objective analyses (Paegle and Horel 1991), for predictability work (Vukicevic and Paegle 1989; Paegle et al. 1997; Miguez-Macho and Paegle 2000, 2001), for idealized global simulations of tropical-extratropical interactions (Buchmann et al. 1995), to study orographically forced regional circulations (Nogues-Paegle et al. 1998; Byerle and Paegle 2003), and for initial data impact investigations of the 1993 “storm of the century” (Miguez-Macho and Paegle 1999a,b).

3. INITIAL STATE ERROR EVOLUTION

MMP demonstrated that the influence of initial state uncertainty is far from saturation after five days of simulation by the Utah model. They studied forecast sensitivity to initial state uncertainty due to different complementary wave groups in the total initial uncertainty. The uncertainty was estimated from the difference of two equally credible analyses of the atmosphere, provided by NCEP-NCAR (T36 truncation) and ECMWF reanalyses of the same state during boreal winter 1993. These analyses, which use the same observations, are very similar over land areas of good observational coverage (see Fig. 1 for 500-mb height and wind analysis differences), but they differ more substantially in regions of poor observations, such as the southern oceans.

In qualitative terms, the spatial structures of analysis differences displayed in Fig. 1, represent the expected geographical distribution of the initial state uncertainty. In particular, the analysis differences are small over well-observed continents and larger over poorly observed regions of the globe. For this study, it is assumed this difference field provides a reasonable estimate of the actual observation uncertainty. The influence of this level of initial state uncertainty is determined by repeating separate forecasts made by the low-resolution UGM initialized with NCEP-NCAR and with ECMWF reanalyses, and studying the evolving difference fields of the predictions. Following MMP, sequences of experimental cases are performed in which separate spectral wave groups are modified in the initial data, and results are normalized by dividing by the variance of the predicted difference

produced by initial state modifications of the entire spectrum. Present results emphasize the response in the meridional wind since this effectively represents the positioning and magnitude of synoptic-scale waves. This quantity also better represents the variability in the Tropics than does the height field.

The results are displayed in Fig. 2, which depicts normalized forecast responses to uncertainties retained in different portions of the global spectrum for the 1993 cases. If the forecasts were extended over a sufficiently long period, error growth would saturate, and all the curves of Figs. 2a and 2b would asymptote to 1.0, and the curves of Fig. 2c would then asymptote to 2.0.

MMP produced the results of Figs. 2a and 2b out to five days (120 h), and noted that sums of normalized uncertainty growth for complementary wave groups approximately equal 1.0 rather than 2.0. They concluded that the first five days of prediction by the Utah model were characterized by slow, linear error growth, which is far from saturation through five days. Within this regime of unsaturated error growth, the effect of changing longwave components of the uncertainty spectrum produces an error contribution that grows more rapidly in a relative sense than does the effect of changing shorter waves of the initial state. This can be deduced from the initial upward trends of the curves in Fig. 2a and the initial downward trend in the curves in Fig. 2b.

The present extension to 14-day predictions provides important modifications of these conclusions. In particular, pronounced growth of the sum of the normalized uncertainty contributions in Fig. 2c occurs after 120 h, when the sums are on the order of 1.1 or less. By 336 h, the sums exhibited in Fig. 2c range from 1.5 to nearly 1.7 suggesting that initial state errors have effectively spread across the full spectrum resolved in the present integrations. Even for this extended prediction the longer-wave uncertainty explains at least as much, or more, of the total error growth than does uncertainty in the shorter waves. Waves 0-15, for example, account for less than 40% of the initial uncertainty in the present experiments in Fig. 2a, but produce about 50% more sensitivity at 14 days (336 h) than do waves 16-42 (Fig. 2b).

The sums of the relative uncertainty in different spectral groups increase toward approximately 1.5-1.7 in Fig. 2c. These curves should asymptote to 2.0 in the limit when errors associated with the chaotic nature of the atmosphere would finally saturate. Simmons and Hollingsworth (2002) suggest that the ECMWF model is close to error saturation after approximately 21 days. They base this conclusion upon the rate at which model solutions initialized on consecutive days diverge. The present experiments are integrated to only 14 days and use a different method to study error saturation, but an extrapolation of the curves in Fig. 2c from the second week shown toward 21 days appears to be consistent with Simmons and Hollingsworth's (2002) conclusion.

The most important limitations to the present conclusions are that they are made using a forecast model truncated at relatively low resolution, and that the differences of NCEP-NCAR and ECMWF analyses, which use the same observations, may not adequately reflect the actual uncertainty of the initial state. Higher-resolution models generally allow larger uncertainty growth because model diffusion coefficients need to increase with coarser resolution to control spectral blocking and to limit the accumulation of energy at the shortest resolvable scales due to nonlinear energy cascade.

It is likely that the present method of initial state uncertainty specification underestimates the actual uncertainty in both large and small scales. In particular, neither analysis contains much amplitude in higher-wavenumber, smaller scale components (wavelengths on the order of 1000 km) and their differences may systematically underestimate the impact of errors at these scales.

White et al. (1999) estimated "errors" of the MRF initial state over the intermountain west of the United States in a region of good radiosonde density. Table 2 of that study suggests that initial rms error values for the wind exceed 4 m s^{-1} in the mid troposphere in a region of reliable observations. These "uncertainties" are estimated from the fit of the initial analyses interpolated to radiosonde observation sites using a horizontal grid corresponding to approximately global wavenumber 100. Presumably, the uncertainties are even larger in regions of sparse observations. The initial data uncertainties (Fig. 1) used in the present low-reso-

lution experiments are smaller than 4 m s^{-1} over most of the globe, and impose smaller initial state uncertainties than were found by White et al. (1999) in data-rich regions.

4. RESOLUTION ENHANCEMENT IN UGM

UGM sensitivity to initial state uncertainty was shown to increase with resolution enhancement in Roman et al. (2004). The purpose of the present chapter is to repeat at doubled horizontal resolution earlier experiments in which the initial state uncertainty was spectrally binned in short-wave and long-wave components.

a. Model

The higher-resolution UGM doubles east-west resolution to include 257 grid points. Fourier series depicting longitudinal variability are now truncated at wavenumber 84 to avoid aliasing instability, and in the north-south direction the number of model nodal points is increased from 82 to 164. The number and location of vertical levels is left unchanged with respect to the wavenumber 42 integrations. Ideally, resolution in all three dimensions should be at least doubled, but the presently enhanced resolution represents the largest model that could be executed for the required number of cases within the timeframe of the study. Even so, computer time limitations restricted the high resolution (wavenumber 84) experiments to a subset of 15 cases between 26 January and 24 February 2004.

b. Initial States

A series of experiments was performed using the NCAR-NCEP reanalyses as well as the GDAS analyses for the 15 selected cases. Enstrophy spectra for these two analyses are displayed in Fig. 3 for a particular day in the Northern Hemisphere winter 2002/03. Enstrophy is the square of the vorticity field, and its spectrum emphasizes shorter waves. The streamfunction is first computed globally from the wind field, and then projected onto spherical harmonics. Globally integrated enstrophy may be expressed as:

$$\int_A (\nabla^2 \Psi)^2 DA = \sum_{mn} (A_n^m)^2 [n(n+1)]^2$$

where *A* is the global area, Ψ is the streamfunction, and A_n^m is the amplitude coefficient of the spherical harmonic component of degree *n* and order *m*. The quantity

$$\left[\sum_m (A_n^m)^2 \right]^{1/2}$$

is plotted against global wavenumber n in Fig. 3, for 30 January 2003 at sigma level 0.3. The highest values are evident in the lowest wavenumbers, or in the longer waves of both analyses. The GDAS analysis (circles) clearly retains more amplitude in global wavenumbers on the order of, or exceeding 30, suggesting that it resolves much more of the sub-synoptic structure than does the NCEP-NCAR reanalysis (solid).

c. Spectral Binning of Initial State Uncertainty

Initial state sensitivity experiments of section 3 are now repeated using NCEP-NCAR renanalyses and the higher-resolution GDAS analyses as initial conditions for the wavenumber 84 UGM. In view of the computational expense of the wavenumber 84 model, the present section presents experiments in which the initial state uncertainty is retained only in waves 0-15, and in the complementary wavenumbers, 16-84, rather than all four spectral “bins” used for the low-resolution experiments.

The importance of higher resolution GDAS initialization to the wavenumber 42 UGM experiments is illustrated in Fig. 4, which shows the time evolution of sigma=0.53 global variances of forecast meridional flow differences produced by initial data changes for the 1993 cases (Fig. 4a) and 2002/ 2003 cases (Fig. 4b). For comparison with 2003 results, Fig. 4a repeats the 1993 results displayed in section 3, using initial analysis changes restricted in the complementary wave groups 0-15 (open circles) and 16-42 (closed circles), normalized by the effect of changing the initial analysis in the completely resolved spectrum. Recall that the 1993 cases utilized NCEP-NCAR and ECMWF reanalyses. Fig. 4a demonstrates that the initial state meridional flow uncertainty is dominated by

short waves, wavenumbers 16-42, but that the uncertainty of the longer waves, wavenumbers 0-15, becomes more important after 12 h, and remains more important for the 14-day (336 h) duration of the experiment. This is consistent with the findings of MMP.

Figure 4b is based on the same model configuration (UGM, wavenumber 42), but presents results using the difference of NCEP-NCAR reanalyses with GDAS analyses for boreal winter 2002/03 to calculate the initial state uncertainty. The conclusions are rather similar to those of the 1993 cases shown in Fig. 4a, with the uncertainty of the longer waves becoming more important after 12 h, but the relative importance of short wave uncertainty begins to approach that of the longer waves towards the end of the 14-day forecast period.

Figure 5 shows the evolution of normalized global variances at sigma=0.53 of forecast meridional flow differences produced by initial data changes for the high-resolution research model for 1993 and 2003 cases. Figure 5a is based on the 17-case sample of 1993 experiments that are identical to those in Fig. 4a, but the results are based on the wavenumber 84 UGM. An important modification of the results due to the increased model resolution in Fig 5a is that the short-wave uncertainty impact exceeds the long-wave impact for the first 24 h, compared with 12 h in Fig 4a, and although the role of long-wave uncertainty is most important after this in the wavenumber 84 experiments, it is not as dominant as in the wavenumber 42 experiments. Figure 5b, which repeats the 2002/03 experiments of Fig 4b but with wavenumber 84 model resolution, suggests that the influence of the shorter wave detail available in GDAS analyses is more important than longer wave detail for the first three days of prediction, and the longer wave uncertainty is more important after this time, but only by a relatively small amount.

The high-resolution experiments indicate that the UGM executed at wavenumber 84, incorporating added detail available from the GDAS analyses, displays significantly more forecast sensitivity to smaller scales of the initial state, particularly in the first three days of prediction, but that error evolution is slightly more sensitive to uncertainties in the larger scales for medium- and long-range prediction. These results modify those suggested by MMP and by experiments described in section 3.

Recent work reported by Tribbia and Baumhefner (2004) also highlights the need for continued research into the relationship between uncertainty scale and error growth. Their investigations of scale interactions and short-term predictability with the NCAR Community Climate Model Version 3 showed that error growth was not described by an inverse cascade, but that initial state uncertainty in the synoptic scales (wavenumbers 10-20) was most important for growth of errors. Although Tribbia and Baumhefner's experiments used a highly sophisticated climate model run at higher resolutions than the UGM, qualitatively the results match those reported here, and point to the importance of detailed broad spectrum analyses for global weather prediction.

5. CONCLUSIONS

This study has investigated predictability using a research global forecast model, and three different estimates of the initial state. Our approach has been to compare the sensitivity of forecasts to model resolution, and to the initial state. The experimental UGM was applied with three analyses: ECMWF and NCEP-NCAR reanalyses for 1993 and 2003, and GDAS analyses for 2003.

Earlier low-resolution experiments by MMP were expanded from 5 to 14 days. Additionally, some experiments were performed with doubled resolution and modified estimates of initial state uncertainty. These experiments resulted in modifications of previous hypotheses regarding the importance to forecast evolution of the uncertainty of long waves relative to the uncertainty of short waves in the initial state. Doubled model resolution incorporated more detail from the GDAS analyses at shorter wavelengths, allowing significantly more forecast sensitivity to the smaller scales of the initial state, particularly in the first few days of prediction. However, uncertainty in the larger scales of the initial state still plays an important role in medium- and long-range forecasts. Such results point to the importance of detailed analyses at all scales for improved global weather prediction.

Our speculations could be checked by repeating the experiments displayed here using a much higher resolution, more sophisticated model for

experimental forecasts and systematically modifying its input and resolution to quantify forecast sensitivity to uncertainty in the initial state.

Acknowledgments. This research was supported by NSF Grants ATM0109241 and ATM0106776 to the University of Utah. The 1993 renalysis data were obtained from the National Centers for Atmospheric Research with assistance from Dr. J. N. Paegle. The 2003 analyses and MRF forecasts were obtained from the National Centers for Environmental Prediction with assistance from Dr. W. James Steenburgh. Invaluable computer assistance was provided by Bryan White.

References

Bath, L. M., M. A. Dias, D. L. Williamson, G. S. Williamson, and R. J. Wolski, 1987: User's guide to NCAR CCM1. Tech. Rep. NCAR/TN-286+IA, 173 pp.

Buchmann, J., L. E. Buja, J. Nogues-Paegle, and J. Paegle, 1995: The dynamical basis of regional vertical motion fields surrounding localized tropical heating. *J. Climate,* **8,** 1217-1234.

Byerle, L. A., and J. Paegle, 2003: Description of the seasonal cycle of low-level flows flanking the Andes and their interannual variability. *Meteorologica,* **27,** 71-88.

Gibson, J. K., P. Kallberg, S. Uppala, A. Nomura, A. Hernandez, and E. Serrano, 1997: ERA description. ECMWF Re-Analysis Project Report Series, No. 1, 58 pp.

Hacker, J. P., E. S. Krayenhoff, and R. B. Stull, 2003: Ensemble experiments on numerical weather prediction error and uncertainty for a North Pacific forecast failure. *Wea. Forecasting,* **18,** 12-31.

Hart, K. A., 2004: An evaluation of high-resolution modeling and statistical forecast techniques over complex terrain. Ph.D. dissertation, University of Utah, 104 pp.

Hartmann, D. L., R. Buizza, and T. N. Palmer, 1995: Singular vectors: The effect of spatial scale on linear growth of disturbances. *J. Atmos. Sci.,* **52,** 3885-3894.

Kalnay, E., and Coauthors, 1996: The NCEP/NCAR 40-Year Reanalysis Project. *Bull. Amer. Meteor. Soc.,* **77,** 437-471.

Lorenz, E. N., 1969: The predictability of a flow which possesses many scales of motion. *Tellus,* **21,** 289-307.

Miguez-Macho, G., and J. Paegle, 1999a: Optimal observation distribution for numerical weather prediction. Preprints, *Third Symp. on Integrated Observing Systems,* Dallas, TX, Amer. Meteor. Soc., 18-23.

-----, and -----, 1999b: Optimal observation distribution for numerical weather prediction. Preprints, *13th Conf. on Numerical Weather Prediction,* Denver, CO, Amer. Meteor. Soc., 23-26.

-----, and -----, 2000: Sensitivity of a global forecast model to initializations with reanalysis datasets. *Mon. Wea. Rev.,* **128,** 3879-3889.

-----, and -----, 2001: Sensitivity of North American numerical weather prediction to initial state uncertainty in selected upstream subdomains. *Mon. Wea. Rev.,* **129,** 2005-2022.

Nicolini, M., K. M. Waldron, and J. Paegle, 1993: Diurnal variations of low-level jets, vertical motion, and precipitation: A model case study. *Mon. Wea. Rev.,* **121,** 2588-2610.

Nogues-Paegle, J., K. C. Mo, and J. Paegle, 1998: Predictability of the NCEP-NCAR reanalysis model during austral summer. *Mon. Wea. Rev.,* **126,** 3135-3152.

Paegle, J., 1989: A variable resolution global model based upon Fourier and finite element representation. *Mon. Wea. Rev.,* **117,** 583-606.

-----, and J. Horel, 1991: The influence of observational uncertainty upon wind-based analyses. Preprints, *Ninth Conf. on Numerical Weather Prediction,* Denver, CO, Amer. Meteor. Soc., 779-

782.

-----, Q. Yang, and M. Wang, 1997: Predictability in limited area and global models. *Meteor. Atmos. Phys.,* **63,** 53-69.

Palmer, T. N., R. Gelaro, J. Barkmeijer, and R. Buizza, 1998: Singular vectors, metrics, and adaptive observations. *J. Atmos. Sci.,* **55,** 633-653.

Rabier, F., E. Klinker, P. Courtier, and A. Hollingsworth, 1996: Sensitivity of forecast errors to initial conditions. *Quart. J. Roy. Meteor. Soc.,* **122,** 121-150.

Reynolds, C. A., P. J. Webster, and E. Kalnay, 1994: Random error growth in NMC's global forecasts. *Mon. Wea. Rev.,* **122,** 1281-1305.

Simmons, A. J., and A. Hollingsworth, 2002: Some aspects of the improvement in skill of numerical weather prediction. *Quart. J. Roy. Meteor. Soc.,* **128,** 647-677.

Thompson, P. D., 1957: Uncertainty of initial state as a factor in the predictability of large scale atmospheric flow patterns. *Tellus,* **9,** 275-295.

Tribbia, J. J., and D. P. Baumhefner, 2004: Scale interactions and atmospheric predictability: an updated perspective. *Mon. Wea. Rev.,* **132,** 703-713.

Vukicevic, T., and J. Paegle, 1989: The influence of one-way interacting lateral boundary conditions on predictability of flow in bounded numerical models. *Mon. Wea. Rev.,* **117,** 340-350.

Warner, T. T., R. A. Peterson, and R. E. Treadon, 1997: A tutorial on lateral boundary conditions as a basic and potentially serious limitation to regional numerical weather prediction. *Bull. Amer. Meteor. Soc.,* **78,** 2599-2617.

White, B. G., J. Paegle, W. J. Steenburgh, J. D. Horel, R. T. Swanson, L. K. Cook, D. J. Onton, and J. G. Miles, 1999: Short-term forecast validation of six models. *Wea. Forecasting,* **14,** 84-108.

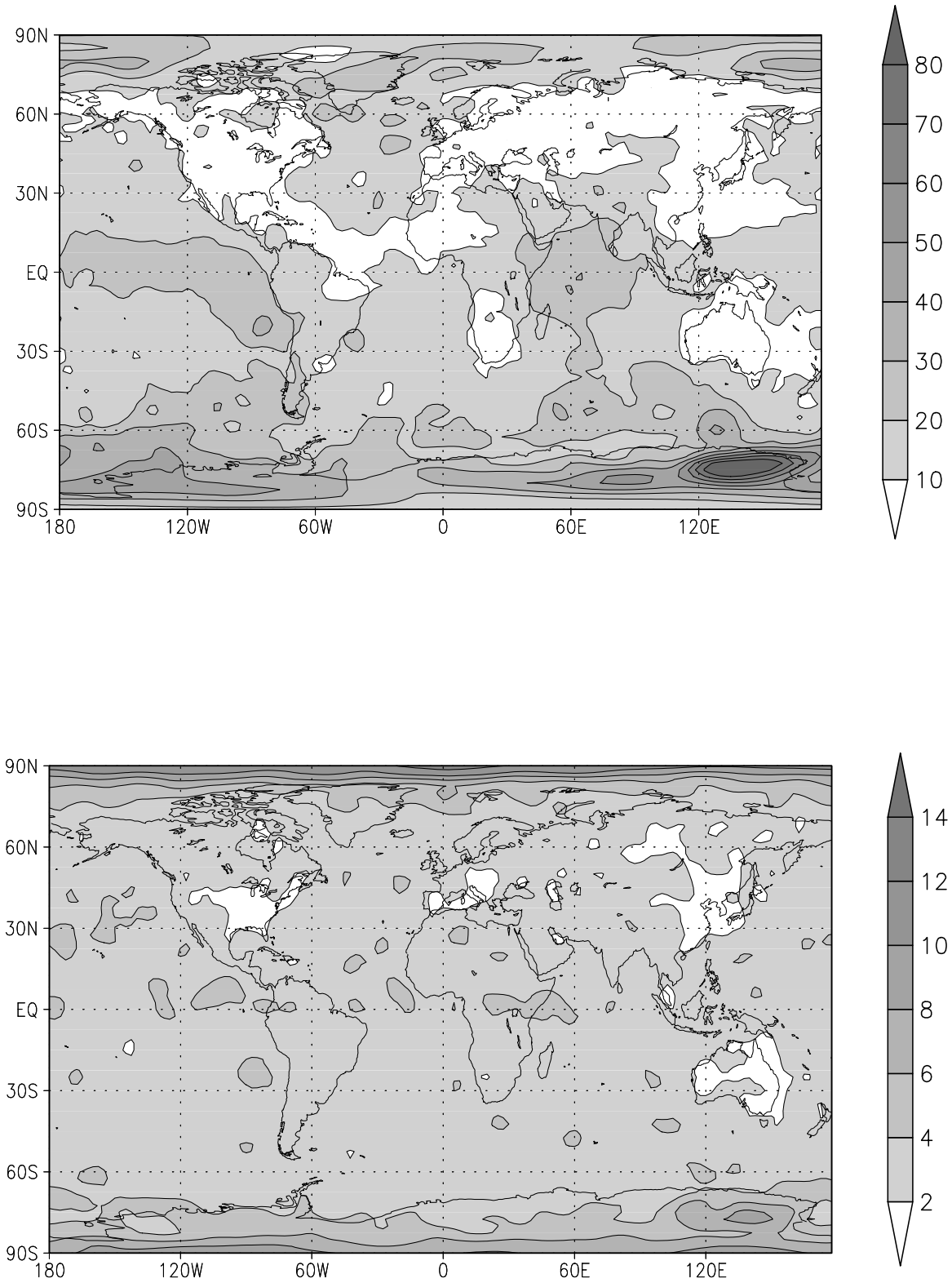

Fig. 1. Initial state 500-mb (top) geopotential height and (bottom) wind rms differences between NCEP-NCAR and ECMWF reanalyses for the 17 cases of 1993. Units are m and m s^{-1}.

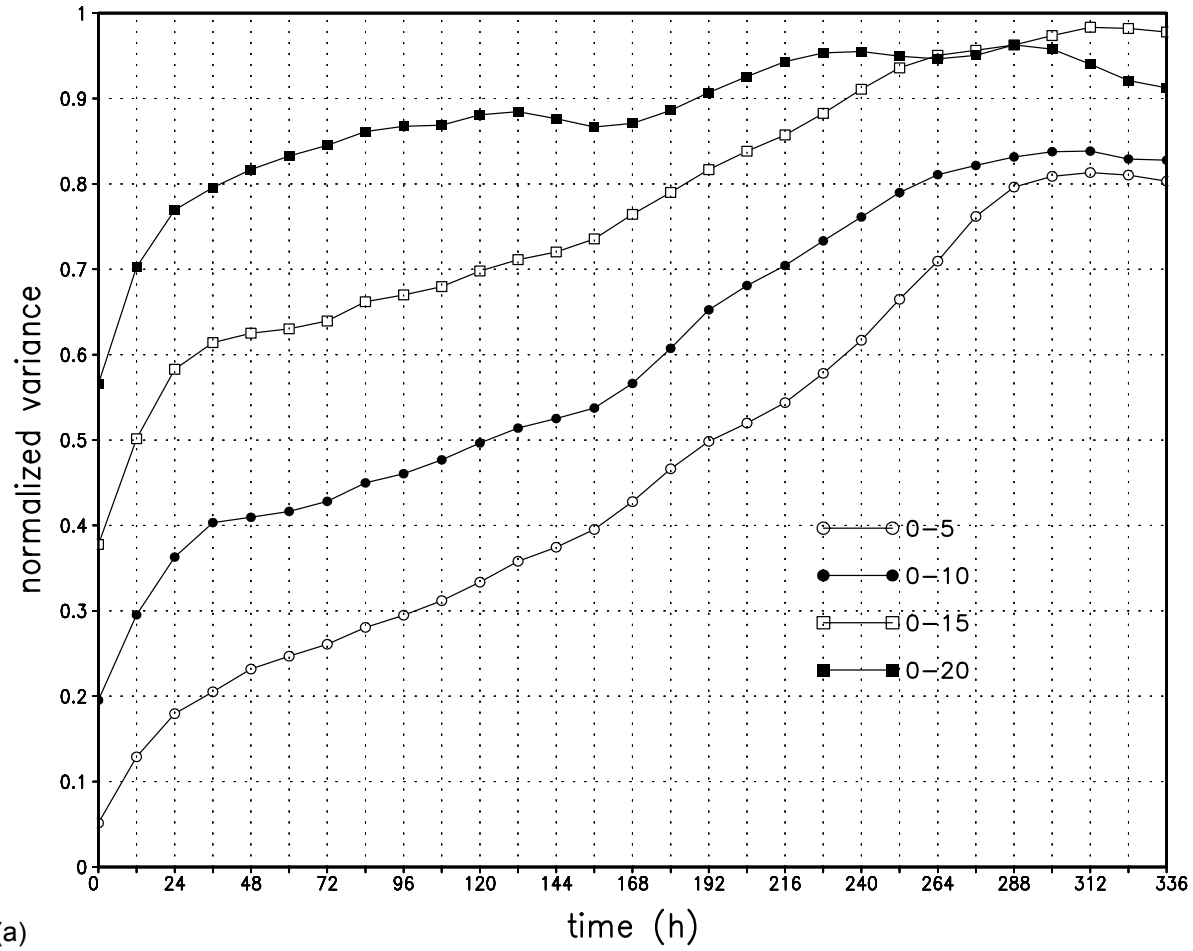

(a)

Fig. 2. Time evolution of global variances at σ = 0.53, of forecast meridional flow differences produced by initial data changes from NCEP-NCAR to ECMWF reanalyses for the 17 cases from boreal winter 1993. (a) Curves show the impact of changing the initial data only for global wavenumbers 0-5 (open circles), 0-10 (closed circles), 0-15 (open squares), and 0-20 (closed squares). (b) Curves display the impact of changing the initial data only for the complementary wavenumbers 6-42 (open circles), 11-42 (closed circles), 16-42 (open squares), and 21-42 (closed squares). Results in both (a) and (b) have been normalized by dividing by the variance of the forecast meridional flow differences produced by the initial state change of the entire spectrum. Sums of complementary wave groups in (a) and (b) are displayed in (c).

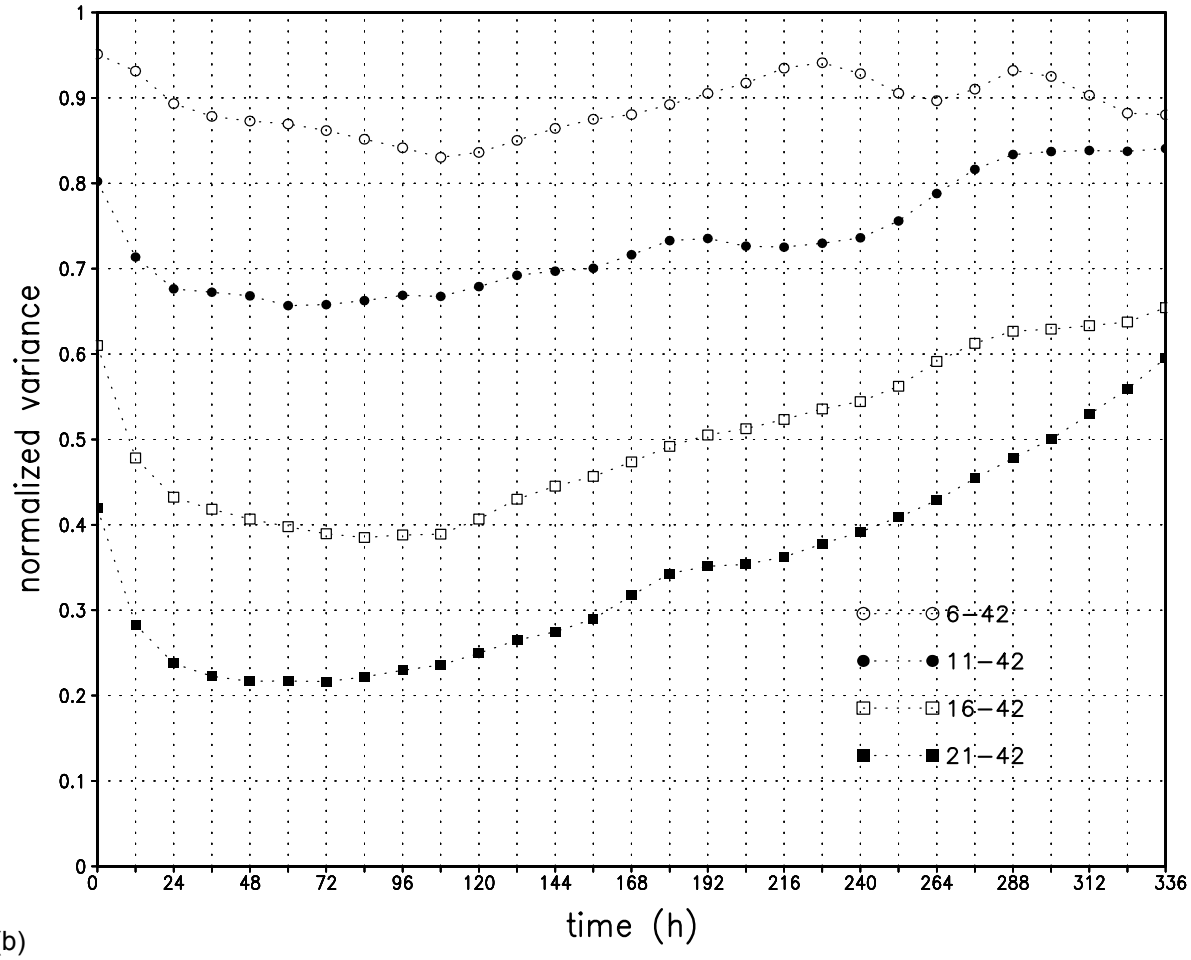

(b)

Fig. 2. (continued)

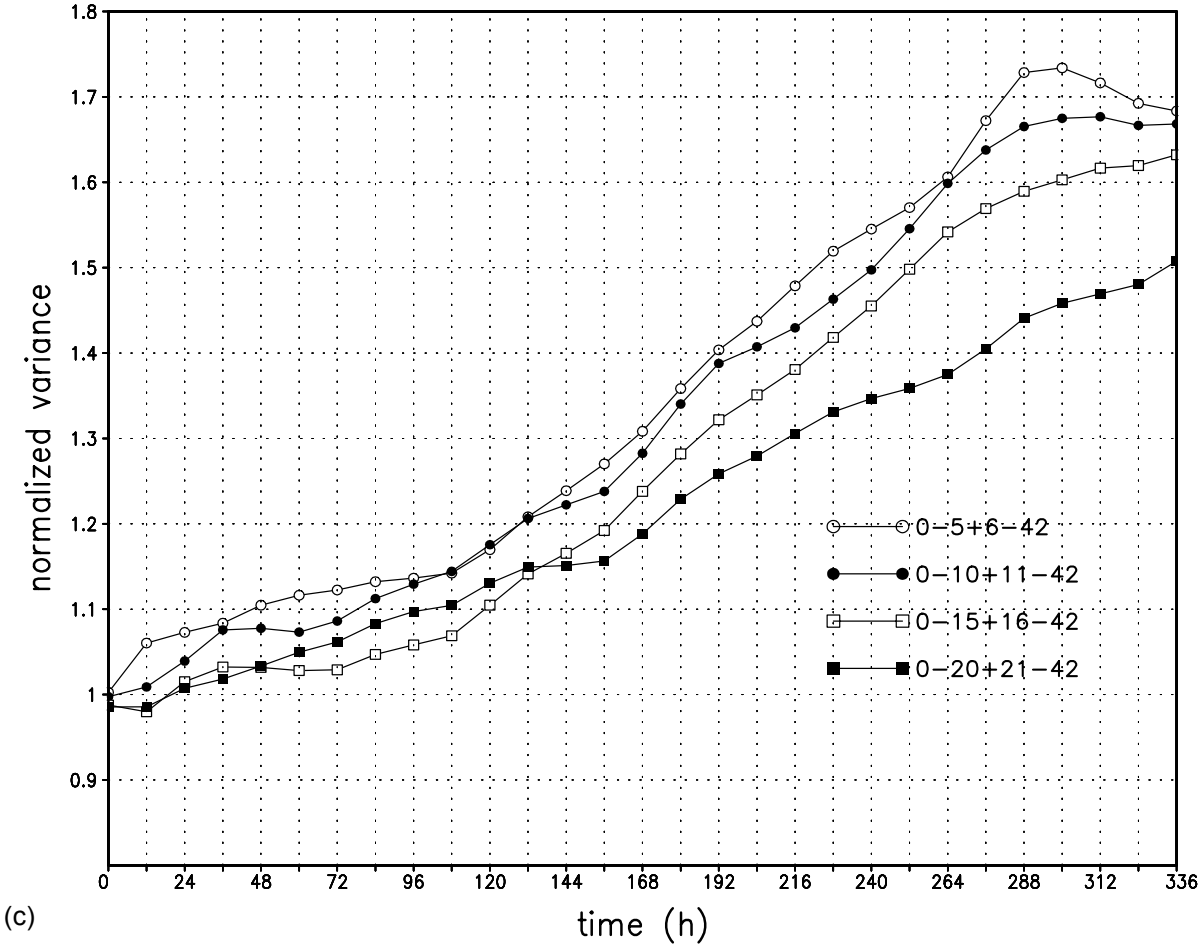

(c)

Fig. 2. (continued)

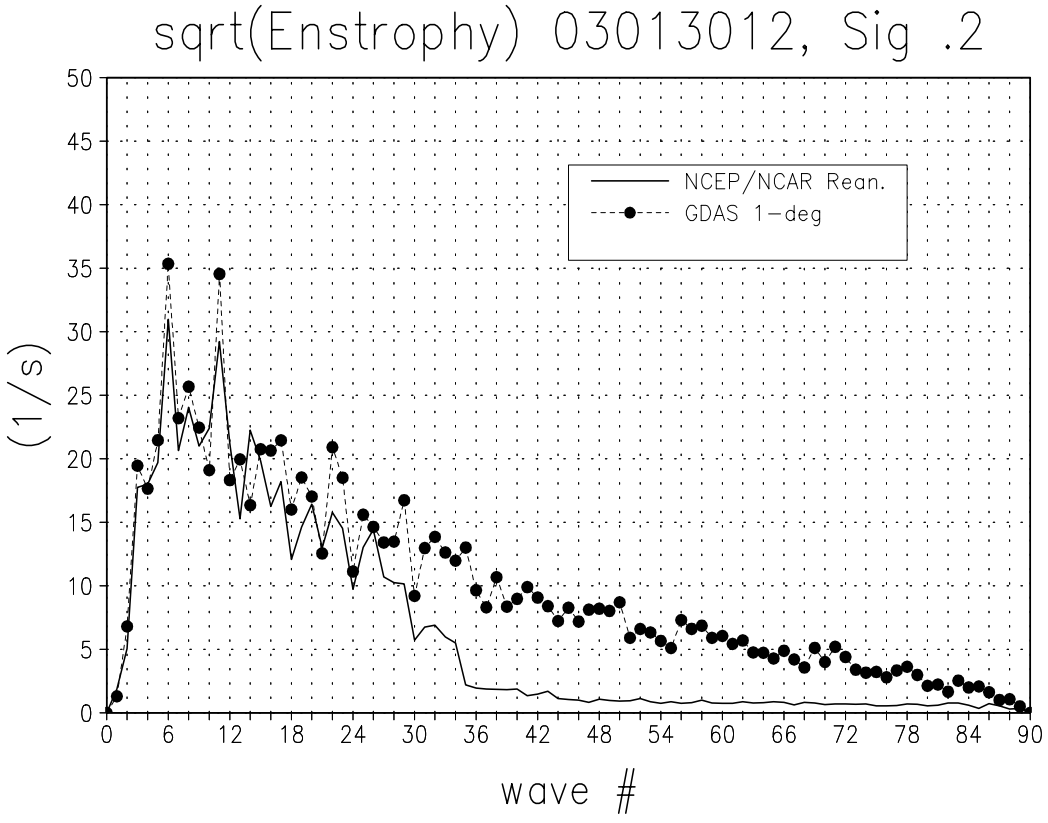

Fig. 3. The square root of the globally-averaged enstrophy spectrum as a function of wavenumber, at 1200 UTC on 30 Jan 2003, for the NCEP-NCAR reanalysis (solid) and GDAS analysis (circles) at sigma level 0.2. Units are s^{-1}.

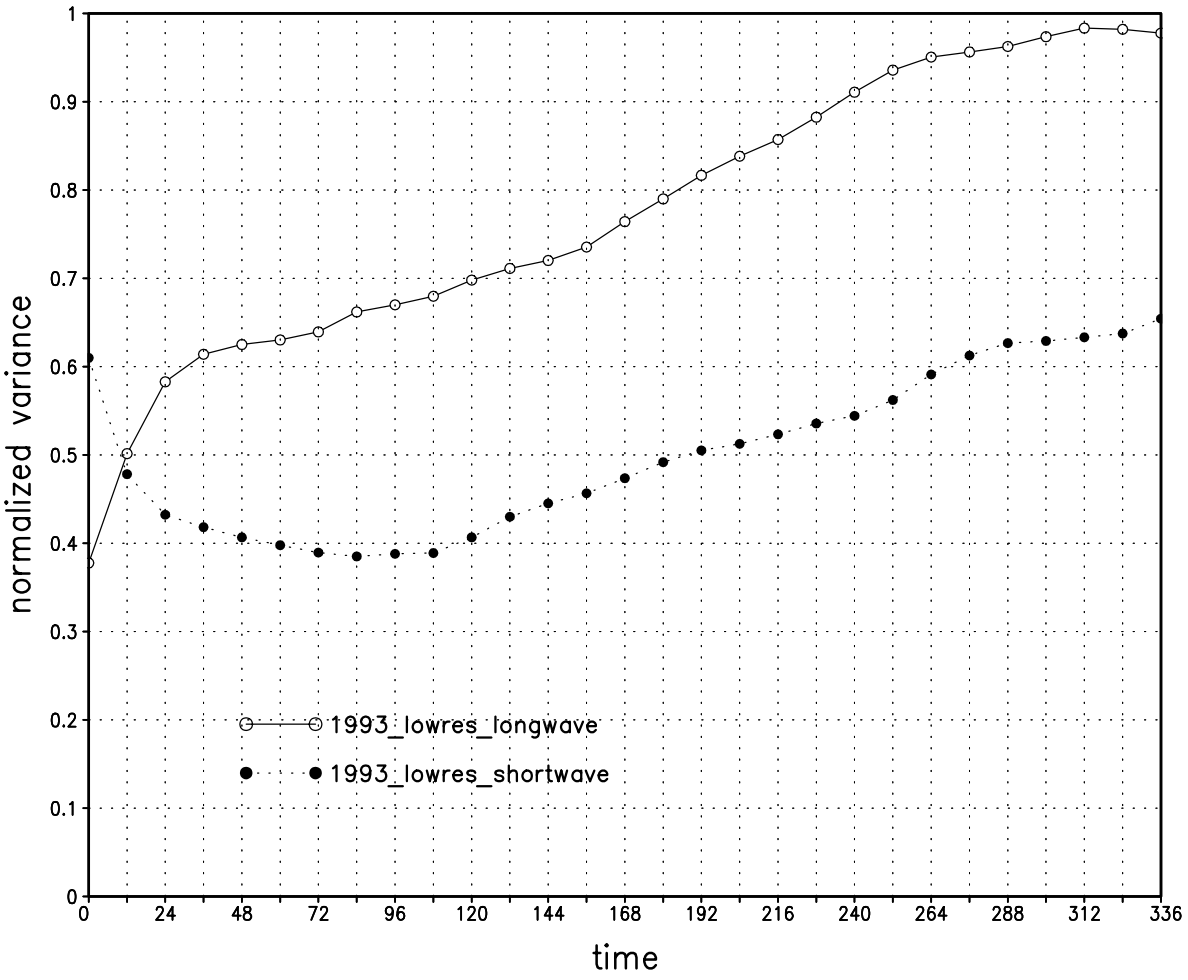

(a)

Fig. 4. Time evolution of normalized global variances at σ=0.53, of forecast meridional flow differences from the wavenumber 42 UGM, produced by initial data changes for global wavenumbers 0-15 (open circles) and for global wavenumbers 16-42 (closed circles). Initial data changes in (a) are from NCEP-NCAR to ECMWF reanalyses for the 1993 cases, and initial data changes in (b) are from NCEP-NCAR to GDAS analyses for the 2003 cases.

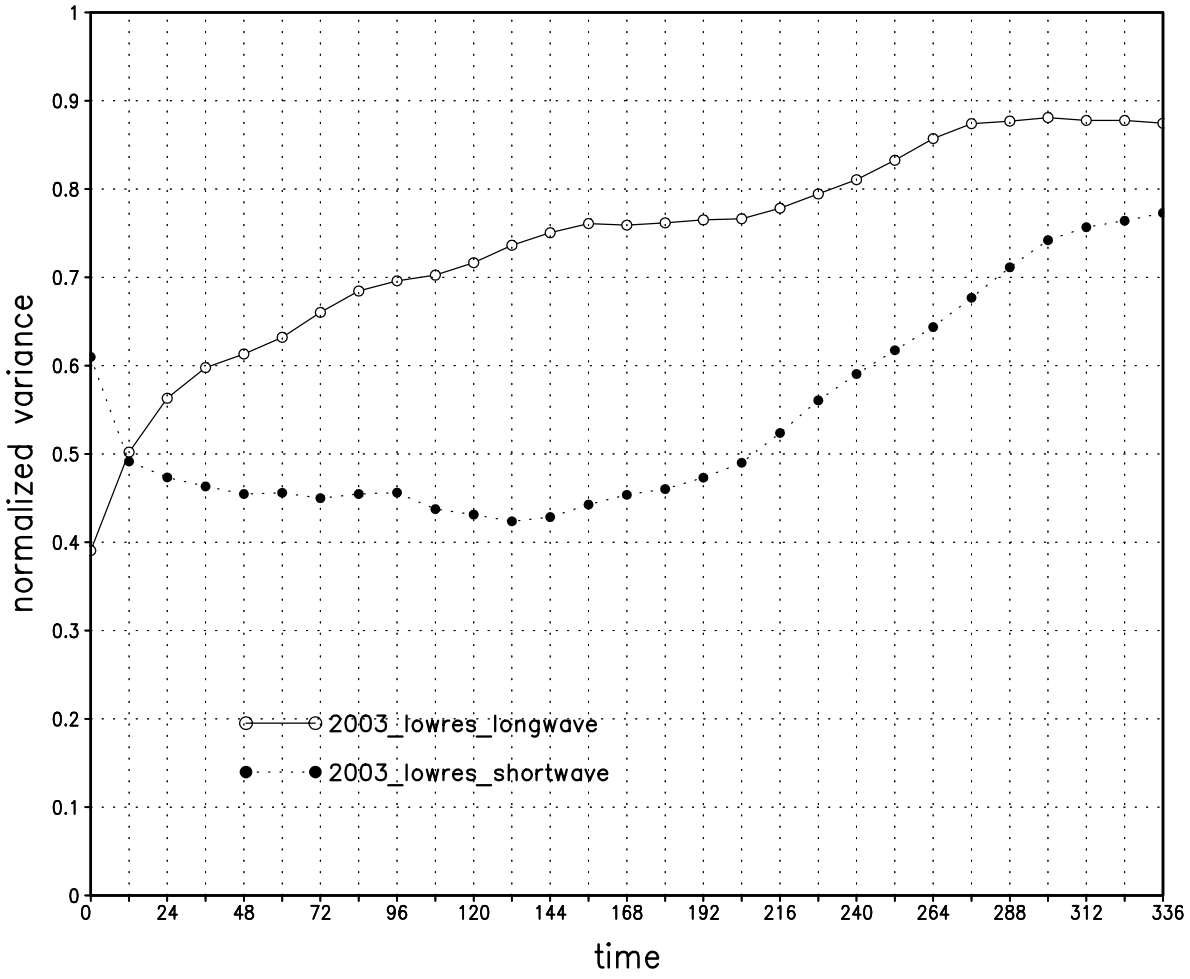

(b)

Fig. 4. (continued)

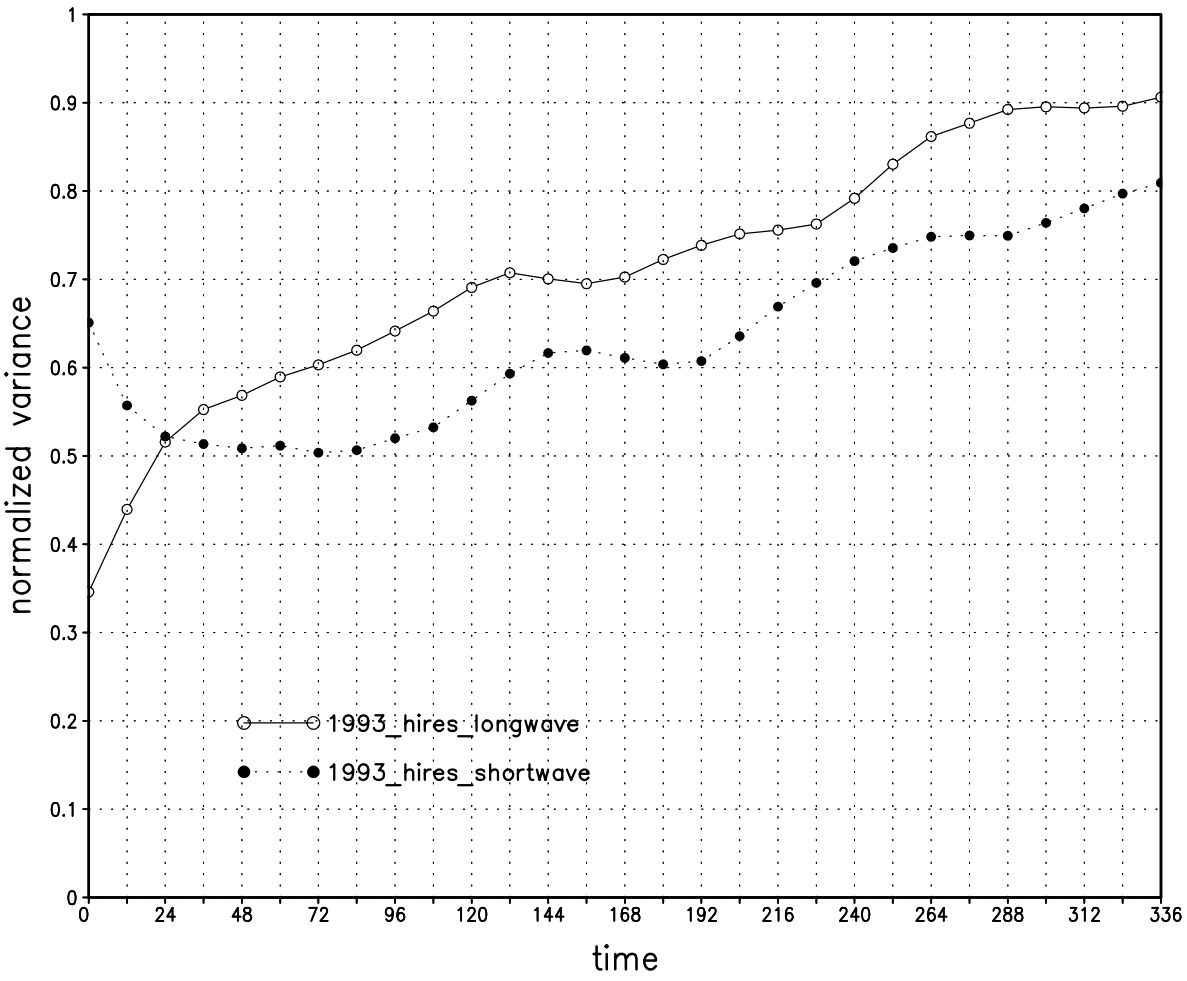

(a)

Fig. 5. Time evolution of normalized global variances at σ=0.53, of forecast meridional flow differences from the wavenumber 84 UGM, produced by initial data changes for global wavenumbers 0-15 (open circles) and for global wavenumbers 16-84 (closed circles). Initial data changes in (a) are from NCEP-NCAR to ECMWF reanalyses for the 1993 cases, and initial data changes in (b) are from NCEP-NCAR to GDAS analyses for the 2003 cases.

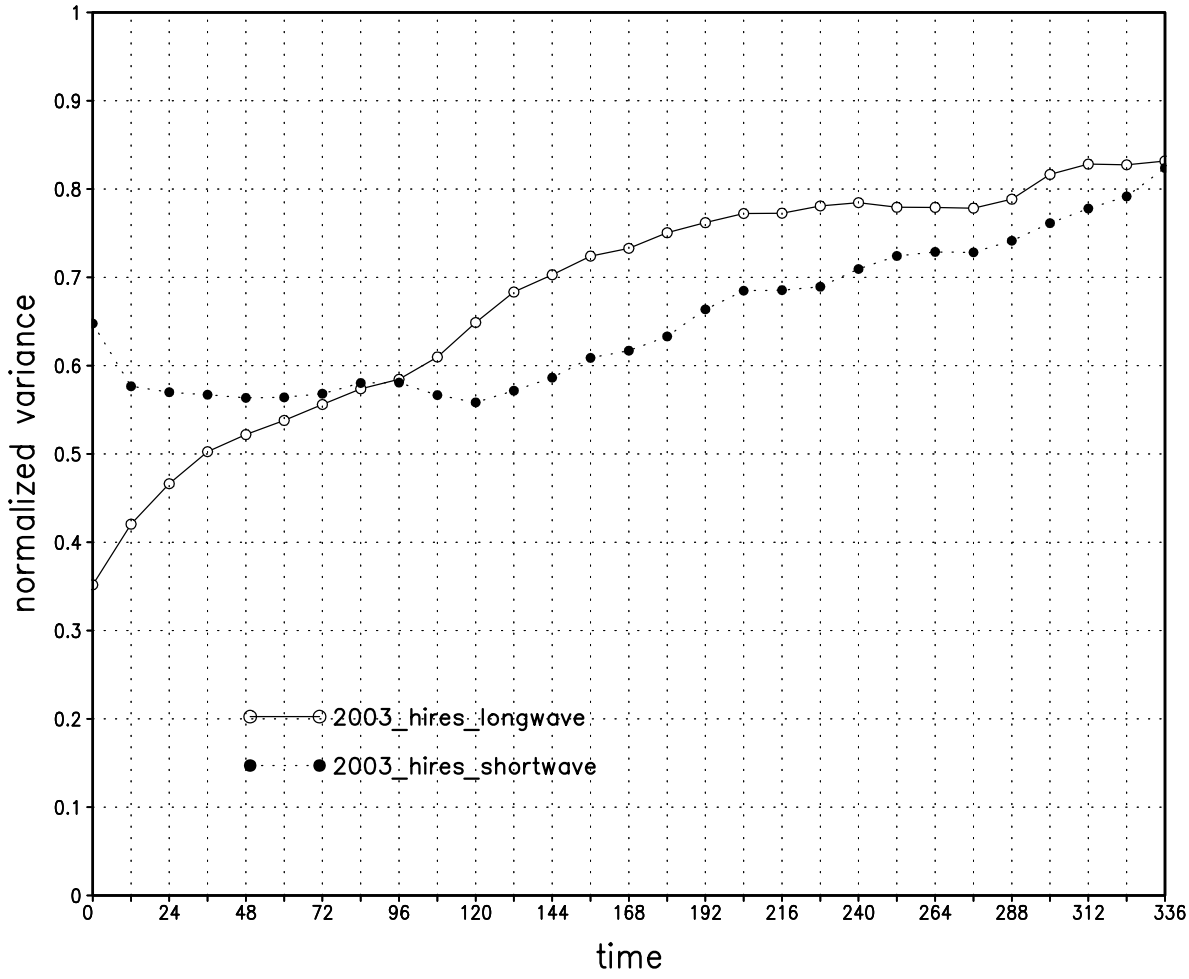

(b)

Fig. 5. (continued)